Determining the Partial Photoionization Cross-Sections of Ethyl Radicals†

B. L. FitzPatrick, M. Maienschein-Cline, and L. J. Butler*

The James Franck Institute and Department of Chemistry, University of Chicago, Chicago, Illinois 60637

S.-H. Lee

National Synchrotron Radiation Research Center, Hsinchu, Taiwan 30076

J. J. Lin

Institute of Atomic and Molecular Sciences, Academia Sinica, Taipei, Taiwan 106 Republic of China

Received: May 17, 2007; In Final Form: June 20, 2007

Using a crossed laser−molecular beam scattering apparatus, these experiments photodissociate ethyl chloride at 193 nm and detect the Cl and ethyl products, resolved by their center-of-mass recoil velocities, with vacuum ultraviolet photoionization. The data determine the relative partial cross-sections for the photoionization of ethyl radicals to form $C_2H_5^+$, $C_2H_4^+$, and $C_2H_3^+$ at 12.1 and 13.8 eV. The data also determine the internal energy distribution of the ethyl radical prior to photoionization, so we can assess the internal energy dependence of the photoionization cross-sections. The results show that the $C_2H_4^+ + H$ and $C_2H_3^+ + H_2$ dissociative photoionization cross-sections strongly depend on the photoionization energy. Calibrating the ethyl radical partial photoionization cross-sections relative to the bandwidth-averaged photoionization cross-section of Cl atoms near 13.8 eV allows us to use these data in conjunction with literature estimates of the Cl atom photoionization cross-sections to put the present bandwidth-averaged cross-sections on an absolute scale. The resulting bandwidth-averaged cross-section for the photoionization of ethyl radicals to $C_2H_5^+$ near 13.8 eV is 8 ± 2 Mb. Comparison of our 12.1 eV data with high-resolution ethyl radical photoionization spectra allows us to roughly put the high-resolution spectrum on the same absolute scale. Thus, one obtains the photoionization cross-section of ethyl radicals to $C_2H_5^+$ from threshold to 12.1 eV. The data show that the onset of the $C_2H_4^+ + H$ dissociative photoionization channel is above 12.1 eV; this result offers a simple way to determine whether the signal observed in photoionization experiments on complex mixtures is due to ethyl radicals. We discuss an application of the results for resolving the product branching in the O + allyl bimolecular reaction.

I. Introduction

Electron bombardment ionization serves as a powerful universal detection method for the study of product branching in unimolecular and bimolecular reactions, but extensive dissociative ionization can complicate the interpretation of observed signals. Whereas low-energy electron impact ionization can substantially reduce dissociative ionization,[1] single-photon ionization is increasingly the method of choice for detecting polyatomic products. To improve the usefulness of this detection method, however, one needs an accurate determination of both the total photoionization cross-sections and the partial photoionization cross-sections for dissociative ionization. Decades of research have established photoionization cross-sections for many stable polyatomic molecules,[2] but characterizing the electron impact[3,4] or photoionization[5−7] (using a method analogous to that in ref 3) cross-sections of radicals and excited-state species presents a more difficult challenge.

Even at threshold, photoionization of a polyatomic radical can result in dissociative ionization,[8,9] and the photoionization efficiency can depend on the internal energy[10] and electronic state[11] of the radical being ionized. Thus, it is important to characterize both the photoionization energy dependence and the internal energy dependence of the partial photoionization cross-sections. This study investigates the low-resolution photoionization of ethyl radicals near 12.1 and 13.8 eV, and it determines the cross-sections for producing both the parent ion ($C_2H_5^+$) and two daughter ions ($C_2H_4^+$ and $C_2H_3^+$) relative to Cl atoms at the higher photoionization energy. Using literature estimates[12,13] for the photoionization cross-section of Cl atoms at 13.8 eV and averaging over the bandwidth of our photoionization source allows us to calculate the absolute cross-section for photoionization of the ethyl radicals. Because our data disperse the nascent neutral ethyl radicals by the kinetic energy imparted in the dissociation of the ethyl chloride photolytic precursor, and thus by the internal energy of the ethyl radical, we can also determine the internal energy dependence, if any, of these photoionization cross-sections. Finally, the data allow us to put prior measurements[14] of the photoion yield curve measured for the photoionization of ethyl radicals at high resolution on a roughly absolute intensity scale, yielding the photoionization cross-section of ethyl radicals to form parent $C_2H_5^+$ from threshold to 1020 Å.

II. Experimental Method

A detailed description of the experimental apparatus appears elsewhere,[15−17] so only the pertinent details are given below. The velocity distributions of the Cl atoms and ethyl radical photofragments of ethyl chloride were measured with the rotating-source, crossed laser−molecular beam apparatus on the 21A1 U9/Chemical Dynamics Beamline at the National Synchrotron Radiation Research Center (NSRRC) located in Hsinchu, Taiwan. A neat beam of ethyl chloride (>99.7% purity,

† Part of the "Giacinto Scoles Festschrift".

* To whom correspondence should be addressed. E-mail: l-butler@uchicago.edu.

10.1021/jp073828h CCC: $37.00
Published on Web 08/31/2007

Aldrich) at room temperature (21 °C) and a backing pressure of 350 Torr was expanded through an Even−Lavie pulsed valve with a 0.4 mm orifice at 50 °C operating at 70 Hz. The speed distribution of the molecular beam was determined using a chopper wheel placed 6.75 cm from the detector. The short flight path necessitated taking considerable care in measuring the timing offsets inherent in the measurement (e.g., the molecular beam passed a chopper slit a quarter revolution after the photodiode sync pulse, so correcting for a rotation frequency of 199 rather than 200 Hz results in a 6.28 μs difference). The peak in the number density distribution of molecular speeds was 730 m/s with a full-width-at-half-maximum of 26%.

A Lambda Physik LPX 220 ArF laser, operating at 193.3 nm, photodissociated the ethyl chloride to produce momentum-matched Cl atoms and ethyl radical photofragments in a 1:1 ratio, allowing us to calibrate the relative photoionization cross-sections. The laser operated at 70 Hz, and the measured pulse energy for each spectrum ranged from 10 to 12 mJ per pulse, well below the saturation level of ethyl chloride. The focused laser beam produced a roughly rectangular pattern 8.5 mm tall by 2.5 mm wide, which intersected the ~3 mm diameter molecular beam at 90° in the interaction region. The recoiling photofragments traveled a neutral flight distance of 10.05 cm to the ionization region, where they were ionized with tunable vacuum ultraviolet (VUV) synchrotron radiation. Photoionization energies were chosen by tuning the U9 undulator gap, and the VUV beam was defined by a 7 mm diameter circular aperture. To interpret bandwidth-averaged cross-sections, we used the resolution of the VUV light source, using the same aperture, determined from measuring sulfur atom spectral lines[18] near 9.6 eV; this gives a full-width-at-half-maximum ΔE divided by the peak energy of 4.2%. Finally, we apply a correction determined by Y.-Y. Lee in unpublished data that spectroscopically recalibrated the nominal photoionization energy calculated from the undulator gap over the range 10−24 eV.[19] Thus, for photoionization spectra taken at an undulator gap of 33 mm in this work, this gap corresponds to a nominal energy of 13.79 eV. However the actual spectrum of the light peaks near 13.77 eV when we apply the energy shift. For photoionization spectra taken at the nominal energy of 12.14 eV, the actual spectrum of the light peaks near 12.08 eV when one applies the correction determined with the smaller aperture. Higher harmonics of the VUV radiation were filtered out using a rare gas filter at about 10 Torr.

After traveling through the ionizing region, the photofragments were ionized and mass selected using an Extrel 1.7 MHz quadrupole mass spectrometer and were counted with a Daly detector. A multichannel scaler recorded the total time-of-flight (TOF) of the photofragments in traveling from the interaction region to the Daly detector. The TOF spectra are forward convolution fit to determine the recoil translational energy distribution for the C−Cl bond fission events that produced ethyl radicals and momentum-matched Cl atoms. Energy conservation then allows us to identify the internal energy distribution of the detected ethyl radicals. The flight times depicted in the figures herein are the sum of the neutral photofragment flight time (from a velocity determined by the vector sum of the center-of-mass velocity and the recoil velocity imparted to the photofragment in the photodissociation) and the ion flight time through the mass spectrometer. The latter is calculated using the apparatus' measured ion flight constant of 5.40 μs amu$^{-1/2}$. All of the TOF spectra and their associated fits are corrected for the 1.54 μs timing offset between the triggering of the multichannel scalar and the later arrival of the laser pulse at the crossing point of the laser and molecular beam.

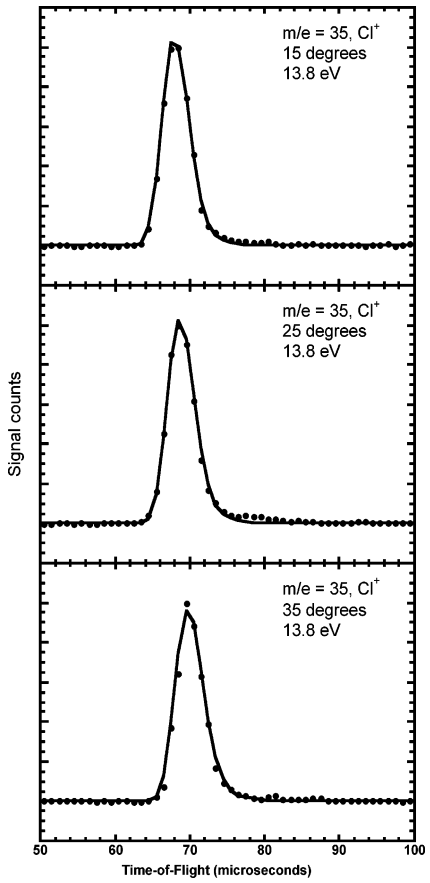

Figure 1. TOF spectrum of the Cl atoms from the photodissociation of ethyl chloride. The data are shown in solid circles, and the forward convolution fit to the data (solid line) is calculated from the total recoil translational energy distribution in Figure 2. All spectra were taken at a photoionization energy centered at 13.8 eV. The angle between the molecular beam and the detector was 15, 25, and 35° in the top, middle, and lower frames, respectively. We do not fit the small feature near the 78 μs flight time becuase its presence depended on the relative timing with the Even−Lavie pulsed valve, so it likely comes from a small fraction of molecular clusters in the beam.

III. Results and Analysis

The data measure the signal from the Cl and ethyl radical photofragments produced in a 1:1 ratio from the photofragmentation of ethyl chloride at 193 nm, detecting the neutral fragments with VUV photoionization. This allows us to determine the ratio between the partial photoionization cross-section of ethyl radicals to its parent ion (m/e = 29 ($C_2H_5^+$)) and the photoionizaton cross-section of Cl atoms near 13.8 eV. Because we disperse the ethyl radical photofragments by the velocity imparted in the C−Cl bond photofission, and thus by their internal energy, we can also assess any internal energy dependence to the measured photoionization cross-sections. The data then determine the relative partial photoionization cross-section of ethyl radicals detected at m/e = 28 ($C_2H_4^+$) and 27 ($C_2H_3^+$) from the dissociative ionization of ethyl radicals at two relatively high photoionization energy ranges near 12.1 and 13.8 eV.

Figure 1 shows the measured TOF spectra of Cl atoms from the 193 nm photodissociation of ethyl chloride, detecting the Cl atoms with VUV photoionization at 13.8 eV with a 4.2% bandwidth. The distribution of energies imparted to recoil kinetic

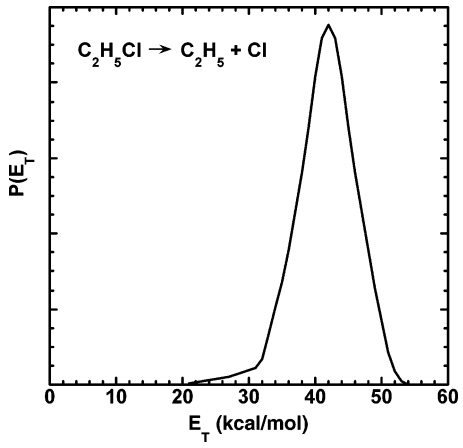

Figure 2. The total recoil kinetic energy distribution for C−Cl bond fission in ethyl chloride photodissociated at 193 nm. This distribution was derived from forward convolution fitting of the Cl atom TOF spectrum shown in Figure 1. It is used to identify the ethyl radical products formed in conjunction with the Cl atoms in the other TOF spectra in this paper and to determine the neutral radical kinematics for interpreting the measured signal in each spectrum.

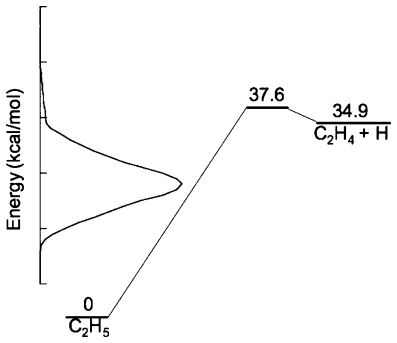

Figure 3. The internal energy distribution (E_{int,C_2H_5}) of the ethyl radicals from C−Cl bond fission in ethyl chloride derived from the measured recoil kinetic energy distribution in Figure 2 using conservation of energy ($E_{int,C_2H_5} = h\nu + E_{parent} - D_0(C-Cl) - E_T = 147.8 + 0.92 - 82.57 - E_T$) is shown superimposed on the zero-point corrected energetics for the $C_2H_5 \rightarrow H + C_2H_4$ reaction calculated at the CCSD-(T)/aug-cc-pvtz level of theory in ref 20. (The calculated energetics agree well with the experimental ΔH at 0 K of 35 kcal/mol for the $C_2H_5 \rightarrow C_2H_4 + H$ reaction.) Radicals formed in conjunction with $Cl(^2P_{1/2})$ would have a lower internal energy by 2.52 kcal/mol. This shows that all of the signals fit in our spectra are from dissociative ionization of stable ethyl radicals. We expect that a significant fraction of this internal energy is in rotation rather than vibration.

energy ($P(E_T)$) between the Cl and ethyl radical photofragments is determined by a forward convolution fit of this spectrum; the resulting $P(E_T)$ is shown in Figure 2. It extends from near 30 to over 50 kcal/mol; therefore, the momentum-matched ethyl radical co-fragments are produced with internal energies ranging from roughly 15 to 35 kcal/mol. We note that, because the C−Cl bond breaks with high partitioning of energy to recoil kinetic energy, a considerable fraction of the internal energy may be in ethyl radical rotational energy, not vibrational energy (an impulsive prediction from the equilibrium geometry of ethyl chloride gives an impact parameter that requires 11.2 kcal/mol to be partitioned to rotational energy when 30 kcal/mol is partitioned to recoil kinetic energy). The lowest measured recoil kinetic energies in the C−Cl bond fission produce ethyl radicals with high internal energies, near the energetic barrier[20] for the radical to dissociate to $H + C_2H_4$, as shown in Figure 3. Figure 4 shows the measured TOF spectra of the ethyl radical co-fragments detected at parent ion ($m/e = 29$) upon VUV photoionization with the same 13.8 eV light source as the Cl

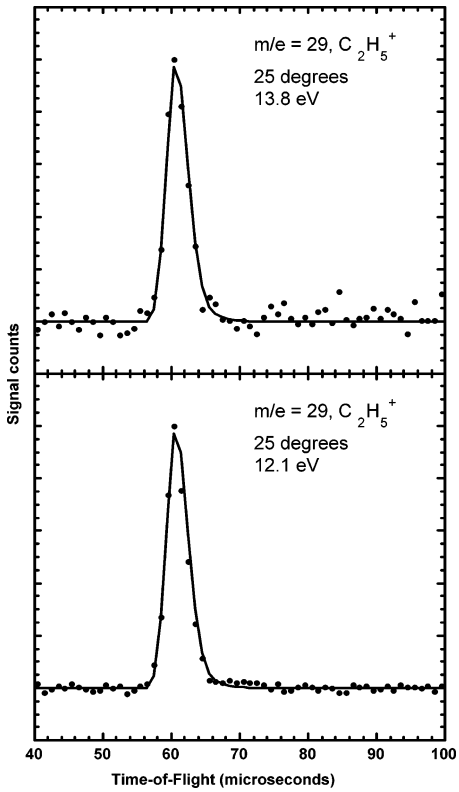

Figure 4. TOF spectrum of the ethyl radical photoproducts detected at $m/e = 29$ ($C_2H_5^+$) with 13.8 eV photoionization (upper frame) and 12.1 eV photoionization (lower frame). The data are shown in solid circles, and the forward convolution fit to the data (solid line) is calculated from the total recoil translational energy distribution in Figure 2 that was derived from the Cl atom spectra in Figure 1. The angle between the molecular beam and the detector was 25°. Each spectrum was accumulated for 200 000 laser shots, and the background was subtracted by taking additional data without the laser light.

atoms in the top frame and tuning the undulator gap to obtain 12.1 eV photoionization energy radiation in the bottom frame. The solid line fit shows the time-of-arrival spectrum of the ethyl radical products predicted from the $P(E_T)$ in Figure 2.

The data in Figures 1 and 4 allow us to determine the photoionization cross-section of ethyl radicals at 13.8 eV, averaged over the bandwidth of the photoionization source relative to that for Cl atoms because the two are produced in a 1:1 ratio in the photodissociation. Using TOF spectra at Cl^+ and $C_2H_5^+$, taken consecutively and detected at 13.8 eV, we integrate the signal in each spectrum, normalizing each to 100 000 laser shots, and divide each integrated signal by a correction factor that accounts for the expected signal due to the three-dimensional scattering kinematics in the photodissociation, the differing transit times through the ionization region due to the neutral fragment velocities, the appropriate Jacobian factors, and the range over which we are integrating the signals (e.g., if we do not integrate the entire range of the signal, the correction factor by which we divide the integrated signal is smaller). We also correct for the fraction (0.7578) of Cl atoms which are ^{35}Cl, because we detect the ethyl radicals that are momentum matched to both isotopes of Cl, but we only detect ^{35}Cl. Because ethyl radicals can, and do, dissociatively ionize at these photoionization energies, we report the result as the partial photoionization cross-section of C_2H_5 to $C_2H_5^+$ ($\sigma_{C_2H_5/C_2H_5^+}$), which is the product of the total photoionization cross-section and the fraction of ionized species that appear at parent ion. Integrating the Cl^+ signal from channels 65 through 76 and the $C_2H_5^+$ signal from channels 57 through 68 and using

the P(E_T) in Figure 2 to make the appropriate corrections for these integration ranges and the differing neutral fragment kinematics for Cl atoms and ethyl radicals, we obtain:

$$\frac{\sigma_{C_2H_5/C_2H_5^+}}{\sigma_{Cl/Cl^+}} = \left(\frac{\text{integrated counts at } C_2H_5^+}{\text{integrated counts at } {}^{35}Cl^+}\right)\left(\frac{75.78}{100}\right)\left(\frac{\text{expected Cl signal}}{\text{expected } C_2H_5 \text{ signal}}\right) = \left(\frac{983}{2955}\right)\left(\frac{75.78}{100}\right)\left(\frac{.0245}{.0195}\right) = 0.32 \quad (1)$$

The uncertainty in this result is roughly 20%. The restricted time at the light source precluded the normal procedures for averaging out drifts in photoionization and molecular beam intensities.

To derive an absolute partial photoionization cross-section for $C_2H_5^+$, we must multiply the ratio above by the bandwidth-averaged photoionization cross-section of Cl atoms. The high-resolution photoionization spectrum[12] of Cl atoms measured from threshold to 750 Å includes multiple sharp and broad resonances, but when averaged over our 4.2% fwhm photoionization source, the cross-section shows little variation near 13.8 eV. (We calculated the bandwidth-averaged cross-section by digitizing the portion of the high-resolution photoionization spectrum in ref 12 from 12.93 to 14.4 eV at energy increments of 0.005 eV and averaging the cross-section over the 4.2% fwhm photoionization source.) Calculating the bandwidth-averaged cross-section of Cl atoms near 13.8 eV from the 1983 experimental photoion yield curve measured by Ruscic and Berkowitz[12] yields a value of 27.9 Mb. However, that work put the measured photoion yield curve on an absolute scale using theoretical predictions for the cross-section in the continuum just beyond the ^1S_o threshold, which at that time were 40.2 Mb. Based on subsequent experimental and theoretical values, Berkowitz[13] recommends a slightly lower cross-section of 34.2 Mb in the continuum beyond the ^1S_o threshold, which corrects our bandwidth-averaged cross-section of Cl atoms to 23.7 Mb at 13.8 eV. Using this correction puts the results in this paper on the same scale as a recent determination of the photoionization cross-sections of vinyl and propargyl radicals.[5] Thus, multiplying our experimentally determined ratio in eq 1 by 23.7 Mb gives an absolute ethyl radical partial photoionization cross-section of 8 ± 2 Mb.

We also took data to determine the partial photoionization cross-sections of ethyl radicals to $C_2H_4^+$ and $C_2H_3^+$, the latter via a well-studied dissociative ionization of ethyl radicals to $C_2H_3^+ + H_2$. Figures 5 and 6 show the measured TOF spectra of the ethyl radical co-fragments detected at $m/e = 28$ and $m/e = 27$ upon VUV photoionization with the same 13.8 eV light source at the Cl atoms in the top frame of each figure and tuning the undulator gap to obtain 12.1 eV photoionization energy radiation in the bottom frame of each figure. The solid-line fit in each shows the TOF spectrum of the ethyl radical products predicted from the P(E_T) in Figure 2. Clearly, at 12.1 eV the dissociative ionization of ethyl radicals to produce $C_2H_4^+$ is not a significant channel, but at 13.8 eV the cross-section for this dissociative ionization process is nearly double the cross-section for producing parent ion and is nearly equal to that for producing $C_2H_3^+$. We calculate the cross-sections for dissociative ionization relative to that for producing parent ion by integrating the $C_2H_4^+$ data from channels 57 to 68 and the $C_2H_3^+$ from channels 56−65, and we make the appropriate corrections for the integration range and the kinematics and other apparatus factors as described in eq 1 above (The ratio of correction factors is not shown in the first equation below, comparing the $C_2H_4^+$ and $C_2H_5^+$ signals, as it is essentially unity). The results for photoionizing with our broad bandwidth centered at 13.8 eV are as follows.

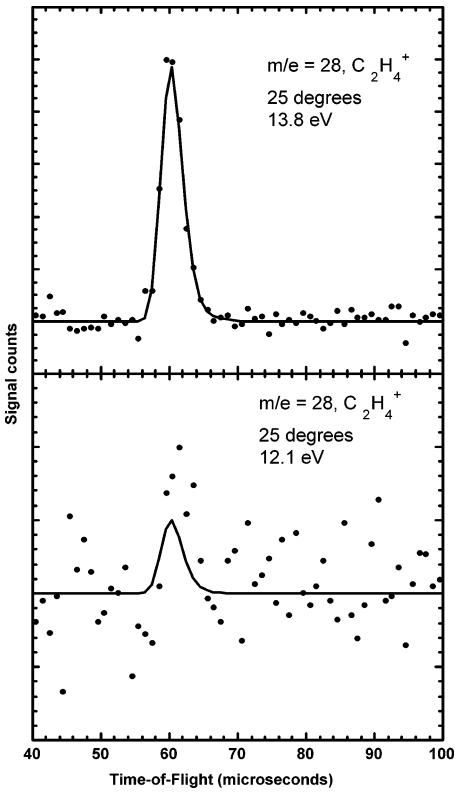

Figure 5. TOF spectrum of the ethyl radical photoproducts detected at $m/e = 28$ ($C_2H_4^+$) with 13.8 eV photoionization (upper frame) and 12.1 eV photoionization (lower frame). The data are shown in solid circles, and the forward convolution fit to the data (solid line) is calculated from the total recoil translational energy distribution in Figure 2 that was derived from the Cl atom spectra in Figure 1. (In the lower frame the fit is shown to indicate where the signal would have appeared.) The angle between the molecular beam and the detector was 25°, Each spectrum was accumulated for 200 000 laser shots, and the background was subtracted by taking additional data without the laser light.

$$\frac{\sigma_{C_2H_5/C_2H_4^+}}{\sigma_{C_2H_5/C_2H_5^+}} = \left(\frac{\text{integrated counts at } C_2H_4^+}{\text{integrated counts at } C_2H_5^+}\right) = \left(\frac{1793}{983}\right) = 1.8 \text{ @ } 13.8 \text{ eV}$$

$$\frac{\sigma_{C_2H_5/C_2H_3^+}}{\sigma_{C_2H_5/C_2H_5^+}} = \left(\frac{\text{integrated counts at } C_2H_3^+}{\text{integrated counts at } C_2H_5^+}\right)\left(\frac{\text{expected signal in } m/e = 29 \text{ integration range}}{\text{expected signal in } m/e = 27 \text{ integration range}}\right) = \left(\frac{1855}{983}\right)\left(\frac{.0195}{.0191}\right) = 1.9 \text{ @ } 13.8 \text{ eV} \quad (2)$$

In contrast, when one uses 12.1 eV photons for the photoionization, the dissociative ionization of ethyl radicals to $C_2H_4^+$ is almost negligible, whereas the $C_2H_3^+$ channel is still significant. The results from integrating the data in the lower frames of Figures 5 and 6 are as follows:

$$\frac{\sigma_{C_2H_5/C_2H_4^+}}{\sigma_{C_2H_5/C_2H_5^+}} = \left(\frac{\text{integrated counts at } C_2H_4^+}{\text{integrated counts at } C_2H_5^+}\right) = \left(\frac{116 \pm 88}{1553}\right) = 0.07 \pm 0.06$$

$$\frac{\sigma_{C_2H_5/C_2H_3^+}}{\sigma_{C_2H_5/C_2H_5^+}} = \left(\frac{\text{integrated counts at } C_2H_3^+}{\text{integrated counts at } C_2H_5^+}\right) \left(\frac{\text{expected signal in } m/e = 29 \text{ integration range}}{\text{expected signal in } m/e = 27 \text{ integration range}}\right) = \left(\frac{1351}{1553}\right) \left(\frac{.0195}{.0191}\right) = .89 \text{ @ } 12.1 \text{ eV} \quad (3)$$

This result provides a way to definitively characterize the signal from the photoionization of ethyl radicals. Ethyl radicals give a good signal at $m/e = 27$, 28, and 29 using 13.8 eV photoionization but only at $m/e = 27$ and 29 using 12.1 eV photoionization. Interestingly, although the appearance of dissociative ionization to $C_2H_4^+$ is clearly strongly dependent on ionization energy, there is not a large dependence on the internal energy of the radical. The fits to all of the spectra above, at the $m/e = 29$ parent and the $m/e = 28$ and 27 daughter ions, are done assuming that the bandwidth-averaged photoionization cross-section of ethyl radicals is independent of the radical's internal energy from 15 to 35 kcal/mol. This assumption closely fits the high signal-to-noise (S/N) $m/e = 29$ spectrum in Figure 4; a poor fit to the spectrum is obtained if one assumes that the photoionization cross-section of ethyl radicals with an internal energy of 35 kcal/mol is twice that of an ethyl radical with an internal energy of 15 kcal/mol. Prior work by Fan and Pratt[21] investigated the internal energy dependence of the 9.67 eV photoionization of ethyl radicals and concluded that there was "essentially no internal energy dependence" in the photoionization cross-section for ethyl radicals produced with internal energies ranging from 0.2 − 1.1 eV. However, if one re-examines the results presented in Figure 7a of that paper, they suggest that the lower internal energy ethyl radicals do indeed exhibit an internal energy dependent photoionization cross-section.

Ruscic et al.[14] measured the high-resolution $C_2H_5^+$ photoion yield curve for ethyl radicals from 1550 to 1020 Å. Because we have determined the absolute photoionization cross-section of ethyl radicals to $C_2H_5^+$ at 13.8 eV, and also collected data at 12.1 eV, we can crudely estimate the photoionization cross-section of ethyl radicals to $C_2H_5^+$ at 12.1 eV from the relative signal intensities, and in this way we provide a point from which to establish an absolute scale for the high-resolution photoion yield curve measured by Ruscic et al. Although there are substantial errors in this estimate described below, this information, even if it is good to a factor of 2, is important as others seek to estimate their photoionization detection sensitivity to ethyl radicals using different photon sources because they are typically narrower in bandwidth and at lower energies than our 13.8 eV source. To roughly determine the photoionization cross-section at 12.1 eV, we compare the integrated signals at these two photoionization energies in our experiments, and we attempt to correct for any long-term drifts in experimental conditions. The photoionization photon flux is nearly the same at 13.8 eV as at 12.1 eV, so it does not require a correction. The integrated signal at $m/e = 29$ increased from 983 counts at 13.8 eV to 1553 counts at 12.1 eV, suggesting the bandwidth-averaged cross-section at 12.1 eV is roughly 16 Mb, but this value is uncorrected for drifts in other experimental conditions over the 5 h period between the two measurements. Therefore, this value should not be trusted to better than 50%. Nevertheless it provides a crude reference point for establishing the partial photoionization cross-section of ethyl radicals to $C_2H_5^+$ near 1020 Å. Unfortunately, the published high-resolution spectrum was plagued by background subtraction issues in this short wavelength region, so, again, the absolute calibration of the ethyl radical partial photoionization cross-section from 1500 to 1020 Å is only roughly determined by this comparison. (We chose 12.1 eV as the second photoionization energy for this study to better characterize the marked onset of the $m/e = 28$ dissociative photoionization channel of ethyl radicals.)

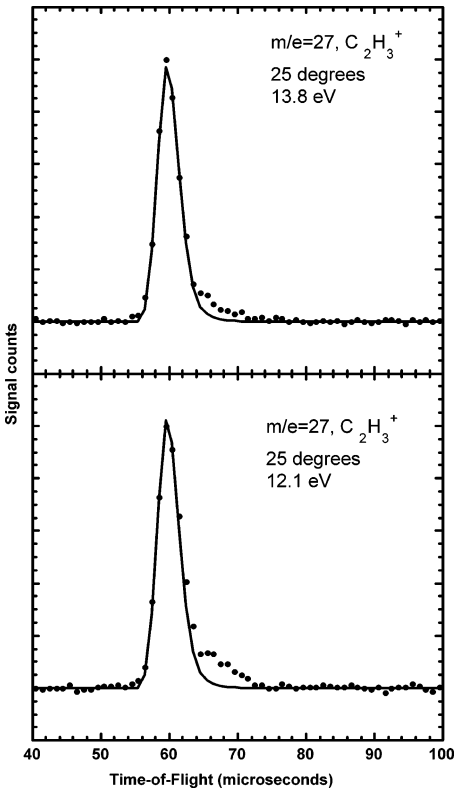

Figure 6. TOF spectrum of the ethyl radical photoproducts detected at $m/e = 27$ ($C_2H_3^+$) with 13.8 eV photoionization (upper frame) and 12.1 eV photoionization (lower frame). The data are shown in solid circles, and the forward convolution fit to the data (solid line) is calculated from the total recoil translational energy distribution in Figure 2 that was derived from the Cl atom spectra in Figure 1. The angle between the molecular beam and the detector was 25°, and the spectra in the upper and lower frames were accumulated for 100 000 and 200 000 laser shots, respectively. The background was subtracted by taking additional data without the laser light. The small shoulder near the 66 μs flight time is not fit or integrated because it not momentum-matched to the reproducible main feature in the Cl atom spectra.

IV. Discussion

The data presented here establish the partial photoionization cross-sections for ethyl radicals to parent ion and two dissociative ionization channels, $m/e = 28$ and 27, at 13.8 and 12.1 eV and the absolute ionization cross-section of ethyl radicals to form $C_2H_5^+$ at 13.8 eV. It also uses data near 12.1 eV to provide a rough calibration of the entire high-resolution $C_2H_5^+$ photoion yield spectrum of ethyl radicals measured by Ruscic et al.[14] from onset to 1020 Å. That high-resolution photoionization spectrum definitively established the adiabatic ionization energy of the ethyl radical as 8.117 ± 0.008 eV (earlier work had reported a higher value as the adiabatic ionization energy reaches a bridged structure[22,23] of the ion that has poor Franck−Condon factors). In addition, the dissociative ionization channel via H_2

loss has long been recognized[24] as an important channel for hydrocarbon species, and early theoretical studies[25] characterized the transition states for 1,1- and 1,2-H_2 elimination from several organic cations. More recent ab initio studies[26] calculate the transition state for 1,1-H_2 elimination from the ethyl cation, reporting an energy barrier of 56 kcal/mol and a loose transition state consistent with the low recoil kinetic energies measured[27,28] for the $C_2H_3^+ + H_2$ products. That paper begins with the remark that H_2 loss is the only unimolecular reaction of ethyl cations, clearly an incorrect statement as the data here examine the H loss channel.

One interesting use for the partial ionization cross-sections presented here is for product identification. For example, recent crossed molecular beam scattering studies[29] of the O + allyl bimolecular reaction sought to investigate the product branching between the H + acrolein product channel and several C−C fission product channels, including CO + C_2H_5 and HCO + ethylene, among others. The study[29] concluded that the H + acrolein channel as well as "one or more" C−C bond fission channels are evidenced in the experimental data. Even though the C−C bond fission products were detected with the lowest practical energy for electron impact detection (17 eV), product identification was hampered by dissociative ionization. Our recent work on this system[30] worked to characterize these product channels by generating a vibrationally excited radical intermediate and detecting the bimolecular reaction products formed from each radical intermediate. We took data at m/e = 29, 28, and 27 at the same two photoionization energies used in this paper to allow us to use the partial ionization cross-sections measured here for the ethyl radical to definitively assess whether the CO + ethyl product channel was contributing to the O + allyl product branching. The TOF distribution[30] of the signals at m/e = 29, 28, and 27 were very similar, suggesting they all come from a product or products with the same or very similar velocity distributions. For instance, the signal at all three masses might be from C_2H_5 products of the CO + ethyl channel or from the two products in the HCO + ethylene product channel, because momentum conservation results in the HCO and ethylene having very similar velocity distributions. We resolve this difficult product identification situation by comparing the relative signals at m/e = 29 and m/e = 28 with the partial ionization cross-sections for ethyl radicals measured here. Whereas ethyl radicals give signal at m/e = 29 and 28 in the rough ratio of 1:2 at 13.8 eV and 1:0.07 ± 0.06 at 12.1 eV, the signals at these masses detected from the dissociation products of this O + allyl reaction intermediate[30] were 4:3 at 13.8 eV and 2:1 at 12.1 eV. The comparison clearly shows that one should not assign the signal at these masses to ethyl radicals because the signal at m/e = 28 at 12.1 eV is far too large as compared to the measured partial ionization cross-sections of ethyl radicals. For this comparison, it was important to have determined in this study that even ethyl radicals formed with an internal energy near the H + ethylene dissociation barrier do not efficiently, dissociatively ionize to m/e = 28 at 12.1 eV.

Acknowledgment. This work was supported by the National Science Foundation under Grant No. CHE-0403471 (Butler). Synchrotron beam time and additional funding were provided by the National Synchrotron Radiation Research Center (NSRRC) and Academia Sinica in Taiwan (Lin). We gratefully acknowledge the assistance in data acquisition at the NSRRC beamline provided by Wen-Jian Huang, Wei-Kan Chen and Chanchal Chaudhuri.

References and Notes

(1) Balucani, N.; Capozza, G.; Leonori, F.; Segoloni, E.; Casavecchia, P. *Int. Rev. Phys. Chem.* **2006**, *25*, 109.
(2) See for example Cool, T. A.; Wang, J.; Nakajima, K.; Taatjes, C. A.; McIlroy, A. *Int. J. Mass Spec.* **2005**, *247*, 18, and references within.
(3) Kitchen, D. C.; Myers, T. L.; Butler, L. J. *J. Phys. Chem.* **1996**, *100*, 5200.
(4) Morton, M. L.; Szpunar, D. E.; Butler, L. J. *J. Chem. Phys.* **2001**, *115*, 204−16.
(5) Robinson, J. C.; Sveum, N. E.; Neumark, D. M. *J. Chem. Phys.* **2003**, *119*, 5311.
(6) Robinson, J. C.; Sveum, N. E.; Neumark, D. M. *Chem. Phys. Lett.* **2004**, *383*, 601.
(7) Sveum, N. E.; Goncher, S. J.; Neumark, D. M. *Phys. Chem. Chem. Phys.* **2006**, *8*, 592.
(8) Harvey, J. N.; Aschi, M. *Phys. Chem. Phys.* **1999**, *1*, 5555.
(9) Krisch, M. J.; McCunn, L. R.; Takematsu, K.; Butler, L. J.; Blase, F. R.; Shu, J. *J. Phys. Chem. A* **2004**, *108*, 1650−6.
(10) See for example Lau, K.−C.; Liu, Y.; Butler, L. J. *J. Chem. Phys.* **2006**, *125*, 144312.
(11) Krisch, M. J.; Miller, J. L.; Butler, L. J.; Su, H.; Bersohn, R.; Shu, J. *J. Chem. Phys.* **2003**, *119*, 176−186.
(12) Ruscic, B.; Berkowitz, J. *Phys. Rev. Lett.* **1983**, *50*, 675.
(13) Berkowitz, J. *Atomic and Molecular Photoabsorption: Absolute Total Cross Sections*; Academic: San Diego, California, 2002.
(14) Ruscic, B.; Berkowitz, J.; Curtiss, L. A.; Pople, J. A. *J. Chem. Phys.* **1989**, *91*, 114.
(15) Wang, C. C.; Lee, Y. T.; Lin, J. J.; Shu, J.; Lee, Y. Y.; Yang, X. J. *Chem. Phys.* **2002**, *117*, 153.
(16) Lee, S.-H.; Lee, Y.-Y.; Lee, Y. T.; Yang, X. *J. Chem. Phys.* **2003**, *119*, 827.
(17) Lin, J. J.; Chen, Y.; Lee, Y. Y.; Lee, Y. T.; Yang, X. *Chem. Phys. Lett.* **2002**, *361*, 374.
(18) Private communication of unpublished results, Lin, J. J.; Lee, S.−H.; Lee, Y.−Y. Jan. 2007.
(19) The unpublished re-calibration measurements of Dr. Yin-Yu Lee in 2006, taken with a smaller aperture of 3 mm, fit the observed shifts to the formula $y = 260.18924 - 5.62356x - 1.21345x^2 + 0.04305x^3 - 0.0013x^4$ for the range of 10 to 24 eV. Here, x is the nominal energy (eV) from the original gap-energy calibration table and y is the corresponding energy shift (in meV) determined from the Lee, Y.−Y. data.[18]
(20) Michael, J. V.; Su, M.−C.; Sutherland, J. W.; Harding, L. B.; Wagner, A. F. *Proc. Combust. Inst.* **2005**, *30*, 965.
(21) Fan, H.; Pratt, S. T. *J. Chem. Phys.* **2005**, *123*, 204301.
(22) A very early calculation of the bridged structure is in Pople, J. A. *Int. J. Mass Spectrom. Ion Processes* **1976**, *19*, 89.
(23) Raghavachari, K.; Whiteside, R. A.; Pople, J. A.; Schleyer, P. V. R. *J. Am. Chem. Soc.* **1981**, *103*, 5649.
(24) Cooks, R. G.; Beynon, J. H.; Caprioli, R. M.; Lester, G. R. *Metastable Ions*; Elsevier: Amsterdam, 1973.
(25) Dewar, M. S.; Rzepa, H. S. *J. Am. Chem. Soc.* **1977**, *99*, 7432.
(26) Uggerud, E. *Eur Mass Spectrom.* **1997**, *3*, 403.
(27) Boyd, R. K.; Beynon, J. H. *Org. Mass. Spectrom.* **1977**, *12*, 163.
(28) Hvistendahl, G.; Williams, D. H. *J. Chem. Soc. Perkin Trans.* **1975**, *2*, 881.
(29) Leonori, F.; Balucani, N.; Capozza, G.; Segoloni, E.; Stranges, D.; Casavecchia, P. *Phys. Chem. Chem. Phys.* **2007**, *9*, 1307.
(30) FitzPatrick, B. L.; Butler, L. J.; Lee, H.-S.; Lin, J. J. manuscript in preparation.